

In situ sulphated $\text{CuO}_x/\text{ZrO}_2$ and $\text{CuO}_x/\text{sulphated-ZrO}_2$ as catalysts for the reduction of NO_x with NH_3 in the presence of excess O_2

Daniela Pietrogiaconi^a, Alessandro Magliano^b, Diana Sannino^b,
Maria Cristina Campa^a, Paolo Ciambelli^b, Valerio Indovina^{a,*}

^aSezione "Materiali Inorganici e Catalisi Eterogenea" dell'Istituto I.S.C. (CNR), c/o Dipartimento di Chimica, Università degli Studi di Roma "La Sapienza", Piazzale Aldo Moro 5, 00185 Rome, Italy

^bDipartimento di Ingegneria Chimica e Alimentare, Università di Salerno, 84084 Fisciano (Salerno), Italy

Received 11 January 2005; received in revised form 24 February 2005; accepted 28 February 2005

Available online 30 March 2005

Abstract

Sulphated catalysts containing the same amount of sulphates ($2.6 \text{ SO}_4 \text{ nm}^{-2}$) and a different amount of copper ($0.3\text{--}3.9 \text{ Cu atoms nm}^{-2}$), Cu/SZ, were prepared by impregnation of sulphated-ZrO₂ with toluene solutions of Cu(acetylacetonate)₂. Sulphated catalysts containing the same amount of copper (0.3 or $2.5 \text{ atoms nm}^{-2}$) and a different amount of sulphates (up to $4.9 \text{ SO}_2 \text{ nm}^{-2}$), Cu/ZS_g, were prepared by sulphation of CuO_x/ZrO₂ (Cu/Z) via the gas-phase. Samples were characterised by Fourier transformed IR spectroscopy. The selective catalytic reduction of NO with NH₃ in the presence of excess O₂ (SCR reaction), the NH₃ + O₂ and the NO + O₂ reactions were studied in a flow apparatus.

Activity and selectivity did not depend on the sulphation method used for catalyst preparation but depended on the amount of copper and sulphate, particularly on the sulphate/copper ratio.

As on Cu/Z, on Cu/SZ Cu^{II} was active for both SCR and NH₃ + O₂ reactions. The presence of covalent sulphates caused lower reducibility of Cu^{II} to Cu^I and higher Lewis acid strength of Cu^I in Cu/SZ than in Cu/Z.

For (i) SCR, (ii) NH₃ + O₂ and (iii) NO + O₂, Cu/ZS_g were less active than the parent Cu/Z. As the sulphate content in Cu/ZS_g increased, the NO yield in the NH₃ + O₂ reaction markedly decreased, thus accounting for the increased selectivity in the SCR reaction. In CuO_x/sulphated-ZrO₂ copper ions were less prone reversibly to undergo the redox process Cu^{II}/Cu^I.

These findings provide new information on the role of copper and sulphate in determining the activity and selectivity for the SCR with NH₃.

© 2005 Elsevier B.V. All rights reserved.

Keywords: NO abatement; SCR; Sulphated-ZrO₂; Supported copper oxide

1. Introduction

The technological, chemical and mechanistic features of the selective catalytic reduction of NO with NH₃ in the presence of O₂ (SCR reaction), with specific attention to VO_x-based catalysts, have been reviewed by Bosh and Janssen [1] and Busca et al. [2]. In power plants, a drawback inherent to the SCR process is the SO₂ present in the flue gas.

On VO_x-based catalysts, in the presence of O₂, SO₂ is oxidized to SO₃. Owing to the concomitant presence of water and unconverted ammonia, SO₃ can give rise to sulphuric acid and ammonium sulphate, resulting in corrosion and deposition of solid by-products downstream from the reactor, where the temperature is lower. To reduce the formation of SO₃ by VO_x, the formulation of commercial catalysts for the SCR has been changed from VO_x/TiO₂ (high VO_x-content) to WO_x, VO_x/TiO₂ or MoO_x, VO_x/TiO₂ (low VO_x-content) [2]. Along with the foregoing undesired effects, SO₃ also has beneficial effects leading to sulphated TiO₂ and sulphated VO_x/TiO₂, both sulphated TiO₂ and

* Corresponding author. Tel.: +39 06 4991 3381; fax: +39 06 490324.

E-mail address: valerio.indovina@uniroma1.it (V. Indovina).

sulphated VO_x/TiO_2 are more active than the parent fresh catalysts for SCR at high temperature [3–9].

For the SCR, unlike sulphated TiO_2 , ZrO_2 sulphated to various extents, up to $2.4 \text{ SO}_4 \text{ nm}^{-2}$, is only slightly more active than pure ZrO_2 . The presence of covalent sulphates does not alone guarantee SCR activity, these species being present in both sulphated TiO_2 and sulphated- ZrO_2 . Active catalysts require the concomitant presence of species possessing redox behaviour, in sulphated TiO_2 , most likely $\text{Ti}^{\text{IV}}/\text{Ti}^{\text{III}}$. Because sulphated- ZrO_2 contains no species endowed with redox behaviour, active ZrO_2 -based catalysts require the presence of copper ($\text{Cu}^{\text{II}}/\text{Cu}^{\text{I}}$).

With ammonia, $\text{CuO}_x/\text{ZrO}_2$ catalysts are active for the SCR reaction. Up to about $2.5 \text{ Cu atoms nm}^{-2}$, namely below the limit at which characterisation showed copper dispersion [10], we found that the activity of $\text{CuO}_x/\text{ZrO}_2$ increased linearly with copper content. On these samples, above 523 K, NH_3 oxidation to NO became prevalent, thus rendering $\text{CuO}_x/\text{ZrO}_2$ unselective [11].

In a recent paper [12], we reported that $\text{CuSO}_4/\text{ZrO}_2$ were also active for SCR and remained highly selective up to 600 K, whereas $\text{CuO}_x/\text{ZrO}_2$ become unselective already at 523 K. On samples with a copper content above 2.5 Cu nm^{-2} , sulphates prevented the formation of copper oxide, thus accounting for their high selectivity. On samples with copper content below 2.5 Cu nm^{-2} , catalytic activity and selectivity depended on a co-operative effect of copper and sulphate [12]. However, because the copper and sulphate content increased in parallel with increasing the CuSO_4 content, we could not determine the specific role of copper, or of sulphates. In the present investigation, to determine the specific role of copper, we inspected the dependence of activity and selectivity on samples with various Cu content ($0.3\text{--}3.9 \text{ Cu atoms nm}^{-2}$), but containing a constant amount of SO_4 . To this aim, we pre-sulphated- ZrO_2 with about $2.6 \text{ SO}_4 \text{ molecules nm}^{-2}$, and impregnated it with toluene $\text{Cu}(\text{acetylacetonate})_2$ solutions of various concentrations. Analogously, to determine the dependence of activity and selectivity on the SO_4 content, we compared samples with various sulphate contents (up to $4.9 \text{ SO}_4 \text{ nm}^{-2}$), but containing a constant amount of copper (0.3 or $2.5 \text{ Cu atoms nm}^{-2}$). These latter samples were prepared by sulphating $\text{CuO}_x/\text{ZrO}_2$ via the gas-phase with $\text{SO}_2 + \text{O}_2$. All samples were characterised by Fourier transformed infrared spectroscopy (FTIR). Along similar lines, Xie et al. [13,14] investigated the simultaneous removal of SO_2 and NO_x using $\text{CuO}_x/\text{Al}_2\text{O}_3$, focussing on the promotion of the SCR activity by SO_2 chemisorption at high temperature [14].

2. Experimental

2.1. Sample preparation

The zirconia support was prepared by hydrolysis of zirconium oxychloride with ammonia, as already described

[15]. The precipitate hydrous zirconium was washed with water until the Cl^- test with AgNO_3 gave no visible opalescence. Before its use as a support, the material was dried at 383 K for 24 h and calcined at 823 K for 5 h. After calcination, the BET surface area of the ZrO_2 support (Z), measured by N_2 adsorption at 77 K, was $53 \text{ m}^2 \text{ g}^{-1}$. XRD spectra showed that Z was in the monoclinic phase.

Sulphated zirconia was prepared by impregnating Z with an aqueous $(\text{NH}_4)_2\text{SO}_4$ solution and calcining at 823 K (SZ(*b*) after calcinations, with $b = 1.0$ or $2.6 \text{ SO}_4 \text{ molecules nm}^{-2}$).

Copper containing catalysts were prepared by three different procedures. In the first procedure, $\text{CuO}_x/\text{ZrO}_2$ were obtained by impregnation of Z with aqueous solutions of $\text{Cu}(\text{NO}_3)_2$, and designated as Cu/Z(*a*), where *a* specifies the analytical copper content. In the second procedure, $\text{CuO}_x/\text{sulphated-ZrO}_2$ were obtained by impregnation of SZ with toluene solutions of $\text{Cu}(\text{acetylacetonate})_2$, and designated as Cu/SZ(*a, b*), where *a* specifies the analytical copper content and *b* the analytical sulphate content. In the third procedure, two Cu/Z(*a*) samples, containing 0.3 or $2.5 \text{ Cu atoms nm}^{-2}$, were sulphated via the gas-phase, by exposing them to a stream containing 1000 ppm SO_2 and 3.6% O_2 in He at 673 K (1000 Ncc/min). Samples were sulphated to different extent by changing the exposure time, from 0.4 to 300 min. These in situ sulphated Cu/Z were designated as Cu/Z(*a*)S_g(*b*), where *a* specifies the analytical copper content and *b* the sulphate content. For comparison, we used portions of $\text{CuSO}_4/\text{ZrO}_2$ catalysts previously prepared and characterised [12]. Samples $\text{CuSO}_4/\text{ZrO}_2$ were obtained by impregnation of Z with aqueous solutions of CuSO_4 , and designated as CuS/Z(*a, b*), where *a* specifies the analytical copper content and *b* the analytical sulphate content. After

Table 1
Catalysts

Starting materials	Catalysts ^a
ZrO ₂	Z
Z + (NH ₄) ₂ SO ₄	SZ(1.0)
Z + (NH ₄) ₂ SO ₄	SZ(2.6)
Z + Cu(nit) ₂	Cu/Z(0.3)
Z + Cu(nit) ₂	Cu/Z(2.5)
Z + Cu(nit) ₂	Cu/Z(4.3)
SZ(1.0) + Cu(acac) ₂	Cu/SZ(0.3, 1.0)
SZ(2.6) + Cu(acac) ₂	Cu/SZ(0.3, 2.5)
SZ(2.6) + Cu(acac) ₂	Cu/SZ(1.6, 2.6)
SZ(2.6) + Cu(acac) ₂	Cu/SZ(3.9, 2.7)
Cu/Z(0.3) + SO ₂ /O ₂ in situ	Cu/Z(0.3)S _g (<i>b</i>), <i>b</i> = 0.4, 0.9, 1.9, 3.5
Cu/Z(2.5) + SO ₂ /O ₂ in situ	Cu/Z(2.5)S _g (<i>b</i>), <i>b</i> = 0.3, 1.4, 2.2, 4.7, 4.9
Z + CuSO ₄	CuS/Z(<i>a, b</i>)

^a For SZ(*b*), the figure in parentheses specifies the analytical SO_4 content. For Cu/Z(*a*), the figure specifies the analytical Cu content. For Cu/SZ(*a, b*), Cu/Z(*a*)S_g(*b*) and CuS/Z(*a, b*), the two figures *a* and *b* specify the analytical Cu and SO_4 content, in that order. Cu/Z(*a*)S_g(*b*) with different SO_4 amount, *b*, were obtained by changing the sulphation time. CuS/Z(*a, b*) were portions of $\text{CuSO}_4/\text{ZrO}_2$ catalysts previously prepared and characterised [12]. All analytical contents are expressed in molecules nm^{-2} .

impregnation, all Cu/Z, Cu/SZ and CuS/Z samples were dried at 383 K and calcined at 823 K.

Copper content was determined by atomic absorption (Varian SpectraAA-30). In samples prepared by impregnation, sulphate content was determined after calcinations at 773 K, by extraction of sulphates with NaOH 1 M, and ionic chromatography of the resulting solution (Dionex 2000i). In samples sulphated via the gas-phase, the sulphate content was measured by monitoring the SO₂ adsorption using a continuous analyser (ABB instrumentation) or by thermogravimetry using a NETZSCH STA209 apparatus, at 5 °C/min heating rate in the range 20–1000 °C. In some selected samples, we measured the sulphate content with both methods: the analytical results were in good agreement. Starting materials for catalyst preparation, catalyst names, analytical copper content and analytical sulphate content are reported in Table 1. All analytical contents are expressed in molecules nm⁻². Surface areas, measured by N₂ adsorption at 77 K, were in the range of 46–50 m² g⁻¹.

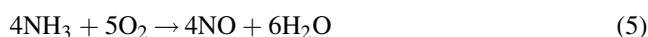
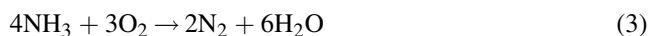
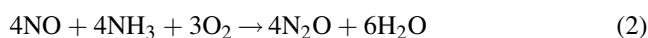
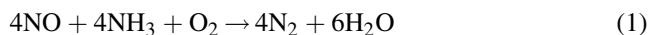
2.2. FTIR measurements

FTIR spectra were recorded at RT on a Perkin-Elmer 2000 spectrometer equipped with an MCT detector, collecting 100 scans at a resolution of 4 cm⁻¹. Powdered materials were pelleted (pressure 1.5 × 10⁴ kg cm⁻²) in self-supporting disks of ca. 16 mg cm⁻² and 0.1–0.2 mm thickness. All samples were placed into an IR quartz cell allowing thermal treatments in vacuo or in a controlled atmosphere. Before experiments, samples were heated in O₂ from RT to 793 K, kept at this temperature for 0.5 h, and evacuated thereafter at the same temperature for 1 h activation procedure. Absorbance spectra were obtained by subtracting the relevant background.

2.3. Catalytic measurements

Catalysts were tested in a flow apparatus consisting of a feeding section, a reaction section and a gas analysis section. High purity gas mixtures, NO/He, NH₃/He, O₂ and He, were fed through mass flow controllers (Hitech) to a fixed bed microreactor, made of two coaxial quartz tubes (i.d. 35 and 16 mm) to allow preheating of feed gas. The microreactor was heated in an electrical oven (Watlow) driven by a temperature controller (Yokogawa PY 27) allowing about 6 cm isothermal length. A K-type thermocouple monitored the temperature of the catalytic bed. The powder catalyst (0.3 g) was pelleted, crushed and sieved to 180–355 μm. Continuous NDIR analysers were used to measure the concentration of reactants and products; Advance Optima Uras 14 (Hartmann & Braun) for NO and N₂O, Ultramat 5E (Siemens) for NH₃. An on-line gas chromatograph (Dani 86.10 HT) equipped with a TCD detector and a double packed column (Alltech CTR 2) was used for N₂, N₂O and O₂ analysis. A P₂O₅ trap avoided interference from the reaction of ammonia with water.

SCR was run feeding a gas mixture containing 700 ppm NO, 700 ppm NH₃, 36,000 ppm O₂, balance He; NH₃ + O₂ with 700 ppm NH₃, 36,000 ppm O₂, balance He and NO + O₂ with 700 ppm NO, 36,000 ppm O₂, balance He. Before catalysis, the sample was treated in airflow at 823 K. Catalytic activity was measured in plug flow conditions at steady-state conversion. Space-time was 0.018 g s cm⁻³ (GHSV = 10⁵ h⁻¹). In all catalytic tests, nitrogen balance was at least 95%. To compare catalytic activity and selectivity of the various catalysts, we assumed that all catalysts brought about the following set of reactions:



The percent selectivity in the NO converted with respect to the NH₃ converted, S_{SCR}, was calculated as S_{SCR} = 100 × (NO converted)/(NH₃ converted). The percent N₂O yield in the SCR reaction and in the NH₃ + O₂ reaction was calculated as 200 × (N₂O produced)/(NH₃ inlet). The percent NO yield in the NH₃ + O₂ reaction was calculated as 100 × (NO produced)/(NH₃ inlet). The rate of the SCR reaction was determined from NO molecules converted *per per* nm² in reactions (1) and (2), that of NH₃ oxidation from NH₃ molecules converted in reactions (3–5), and that of NO oxidation from NO molecules converted in the NO + O₂ reaction. Apparent activation energies (E_a/kJ mol⁻¹) were calculated from Arrhenius plots in the temperature range yielding <40% conversion.

3. Results and discussion

3.1. FTIR characterisation of sulphates

After activation, spectra of all sulphated samples consisted of several bands in the 1200–900 cm⁻¹ region (1200, 1060, 1034, 990, 925 and 900 cm⁻¹), typical of the ν_{S-O}, and a complex absorption in the 1420–1350 cm⁻¹ region, typical of the ν_{S=O} of covalent organic-like sulphates, previously observed by others and assigned to tridentate sulphates carrying a single S=O oscillator (ν_{S=O} up to 1400 cm⁻¹) and poly-nuclear sulphates (ν_{S=O} at ν ≥ 1400 cm⁻¹) [16–18]. The overall intensity of these bands increased with the sulphate content. On CuS/Z, Cu/SZ and Cu/ZS_g containing copper and sulphates in a large amount, ionic sulphates also formed, as reported below.

3.1.1. The dependence of the sulphate type on the sulphate amount and on the copper amount

In samples with a constant copper amount (0.3 or 2.5 Cu atoms nm⁻²), as the SO₄ content increased, the ν_{S=O} wavenumber increased in parallel, indicating an increased

covalent character of sulphates. As an example, the $\nu_{\text{S=O}}$ band maximum was 1370 cm^{-1} on Cu/Z(0.3)S_g(0.4), 1380 cm^{-1} on Cu/SZ(0.3, 1.0) and 1400 cm^{-1} on Cu/SZ(0.3, 2.5). Because the type of sulphate and that of copper do not depend on the sulphation method [19], the comparison included samples prepared by various sulphation methods. An analogous increase in $\nu_{\text{S=O}}$ with an increasing SO₄ content was observed by others on sulphated-ZrO₂ and ascribed to a parallel increase in the ratio of poly-nuclear to mononuclear sulphates [18].

On Cu/SZ(0.3, 2.5) and Cu/SZ(1.6, 2.6), containing the same amount of sulphate but a different amount of copper, the position (about 1400 cm^{-1}) and the intensity of the $\nu_{\text{S=O}}$ band almost matched.

On Cu/SZ(3.9, 2.7), this sample containing the same amount of sulphate, but a larger amount of copper than the two aforementioned samples, and on Cu/Z(2.5)S_g(2.2), Cu/Z(2.5)S_g(4.7) and Cu/Z(2.5)S_g(4.9), all these samples containing copper and sulphates in large amounts, the $\nu_{\text{S=O}}$ band was less intense and occurred at a lower wavenumber (1380 cm^{-1}), indicating a decreased covalent character of sulphates. On all these samples, in addition to covalent sulphates, ionic sulphates also formed, as indicated by the presence of an intense absorption in the $1250\text{--}1100\text{ cm}^{-1}$ region (spectra not shown). A similar intense absorption from ionic sulphates also formed on anhydrous CuSO₄ [20] and on in situ sulphated CuO [21]. The presence of copper and sulphates in large amounts caused a decrease in the number of Zr^{IV} surface sites available to anchor covalent sulphates. As a consequence,

ionic sulphates formed together with a decreased amount of covalent sulphates.

3.2. FTIR characterisation of copper species

On all samples, in addition to the band of Zr^{IV}-CO species in the region $2230\text{--}2170\text{ cm}^{-1}$ [22], CO adsorption at RT yielded a complex absorption in the region $2160\text{--}2115\text{ cm}^{-1}$, assigned to Cu^I-CO species, and weak bands in the region $1650\text{--}1500\text{ cm}^{-1}$, assigned to the asymmetric ν_{OCO} of carbonates [10]. On sulphated samples with Cu content $\geq 1.6\text{ atoms nm}^{-2}$, a shoulder at about 2180 cm^{-1} appeared, assigned to the ν_{sym} of a Cu^I-(CO)₂ species, whose ν_{asym} was obscured by the intense broad-peak of monocarbonyls at $2160\text{--}2115\text{ cm}^{-1}$ [19].

On all sulphated samples, CO adsorption shifted the $\nu_{\text{S=O}}$ complex band to a lower wavenumber and resolved it into various components (1375 , $1340\text{--}1355$ and $1300\text{--}1330\text{ cm}^{-1}$, spectra not shown). We attribute this $\nu_{\text{S=O}}$ shift to side interactions of surface sulphates with adjacent carbonyl species.

3.2.1. The dependence of copper Lewis acid strength on the amounts of sulphate and copper

On Cu/Z, the Cu^I-CO species formed at about 2115 cm^{-1} [10], whereas on CuS/Z, Cu/SZ and Cu/ZS_g, they formed at a higher wavenumber, depending on the amount and type of covalent sulphates, as reported in the next paragraph. The shift to higher wavenumber of the Cu^I-CO band reflected the presence of copper species endowed with a higher Lewis

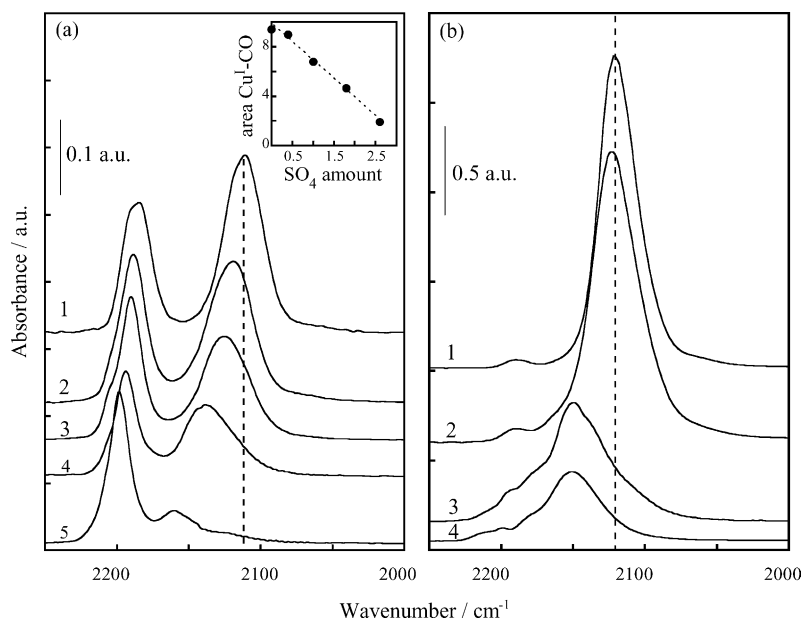


Fig. 1. FTIR spectra after CO adsorption at RT (80 Torr) on samples with the same copper content, 0.3 a) or 2.5 atoms nm^{-2} (b) and different sulphate content. (a) Cu/Z(0.3) (spectrum 1), Cu/Z(0.3)S_g(0.4) (spectrum 2), Cu/SZ(0.3, 1.0) (spectrum 3), Cu/Z(0.3)S_g(1.9) (spectrum 4) and Cu/SZ(0.3, 2.5) (spectrum 5). Inset: integrated intensity (area/ cm^{-1}) of the Cu^I-CO bands as a function of the SO₄ content. (b) Cu/Z(2.5) (spectrum 1), Cu/Z(2.5)S_g(0.3) (spectrum 2), CuS/Z(2.3, 1.9) (spectrum 3) and Cu/Z(2.5)S_g(4.9) (spectrum 4).

acid strength, due to the electron withdrawing effect of nearby covalent sulphates. Analogously, on Cu/Z, the Zr^{IV} -CO species formed at 2191 and at 2185 cm^{-1} [10], whereas on CuS/Z, Cu/SZ and Cu/ZS_g they formed at a higher wave number (2210 and 2200 cm^{-1}), indicating the involvement of Zr^{IV} endowed with higher Lewis acid strength.

On samples with a constant copper amount (0.3 or 2.5 Cu atoms nm^{-2}), the position of the Cu^I -CO band depended on the sulphate content. In particular, on samples containing 0.3 Cu atoms nm^{-2} , as the sulphate content increased, the Cu^I -CO band shifted progressively to a higher wavenumber, from 2111 cm^{-1} in Cu/Z(0.3) to 2160 cm^{-1} in Cu/SZ(0.3, 2.5) (Fig. 1a). On samples containing 2.5 Cu atoms nm^{-2} , the Cu^I -CO band occurred at 2119 cm^{-1} in both Cu/Z(2.5) and Cu/Z(2.5)S_g(0.3), and shifted to a higher wavenumber in CuS/Z(2.3, 1.9) and in Cu/Z(2.5)S_g(4.9) (2151 cm^{-1}) (Fig. 1b). The shift indicated an increased Lewis acid strength of Cu^I sites. Because the type of sulphate and that of copper did not depend on the sulphation method [19], the comparison included samples prepared by various sulphation methods.

On samples Cu/SZ(0.3, 2.5) and Cu/SZ(1.6, 2.6), containing the same amount of sulphate, but a different amount of copper, the Cu^I -CO band position occurred at the

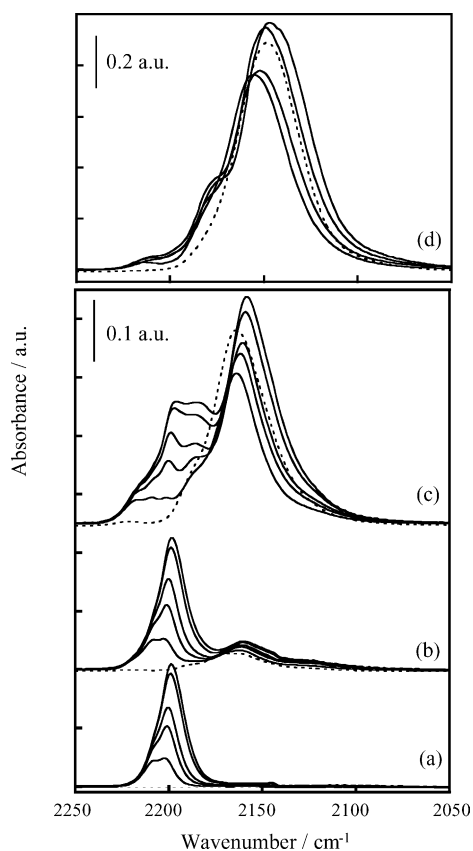


Fig. 2. FTIR spectra after CO adsorption at RT at increasing CO pressure (from 0.2 to 80 Torr) and after evacuation at RT (dotted lines) on Cu/SZ samples. Samples: SZ(2.6) (a), Cu/SZ(0.3, 2.5) (b), Cu/SZ(1.6, 2.6) (c) and Cu/SZ(3.9, 2.7) (d).

same wavenumber (about 2157 cm^{-1}) (Fig. 2b and c), because of the presence of the same type and amount of covalent sulphates. On Cu/SZ(3.6, 2.7), the Cu^I -CO band occurred at a lower wave number (about 2147 cm^{-1}) (Fig. 2d), because of the concomitant presence of ionic sulphates which caused covalent sulphates to form in a lower amount.

On all samples, irrespective of the sulphation method, the Lewis acid strength of copper, $\nu_{Cu(I)-CO}$, paralleled the covalent character of sulphates, $\nu_{S=O}$ (Fig. 3). A similar correlation between $\nu_{Cu(I)-CO}$ and $\nu_{S=O}$ has been reported for CuO_x/Al_2O_3 sulphated via the gas-phase [23].

3.2.2. The dependence of Cu^{II} reducibility on the amounts of sulphate and copper

We will examine first the reduction of Cu^{II} upon CO adsorption at RT. As it did on Cu/Z [10], CO adsorption at RT on CuS/Z, Cu/SZ and Cu/ZS_g caused the reduction of Cu^{II} to Cu^I and the simultaneous formation of Cu^I -CO and carbonates, $2Cu^{II} + 3CO + 2O^{\ominus} \rightarrow 2Cu^I-CO + CO_3^{\ominus}$. In agreement with previous results on Cu/Z, no Cu^{II} carbonyls formed on CuS/Z, Cu/SZ and Cu/ZS_g, because Cu^{II} carbonyls are unstable at RT [10,24]. On Cu/Z, the integrated intensity of Cu^I -CO was proportional to that of carbonates (Fig. 8 in Ref. [10]), demonstrating that carbonates arose from Cu^{II} reduction. Cu^{II} reduced to Cu^I also on CuS/Z, Cu/SZ and Cu/ZS_g. These samples contained low amounts of carbonates, because the presence of surface sulphates hindered CO_2 adsorption.

In samples with a constant amount of copper (0.3 or 2.5 Cu atoms nm^{-2}), the Cu^I -CO band was less intense in sulphated than in unsulphated samples. In samples containing 0.3 Cu atoms nm^{-2} , as the sulphate content increased, the Cu^I -CO band decreased linearly (Fig. 1a and inset). In samples containing 2.5 Cu atoms nm^{-2} , the Cu^I -CO band was nearly equally intense in Cu/Z(2.5) and Cu/Z(2.5)S_g(0.3), and in samples with higher sulphate content

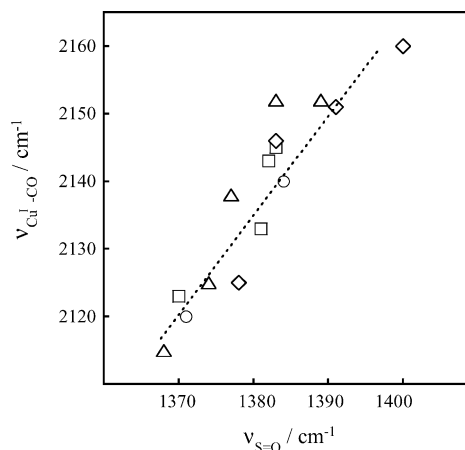


Fig. 3. The Lewis acid strength of copper sites ($\nu_{Cu(I)-CO}$) as a function of the covalent character of sulphates ($\nu_{S=O}$). Samples: Cu/Z(0.3)S_g (○), Cu/Z(2.5)S_g (□), Cu/SZ (◇) and CuS/Z (△).

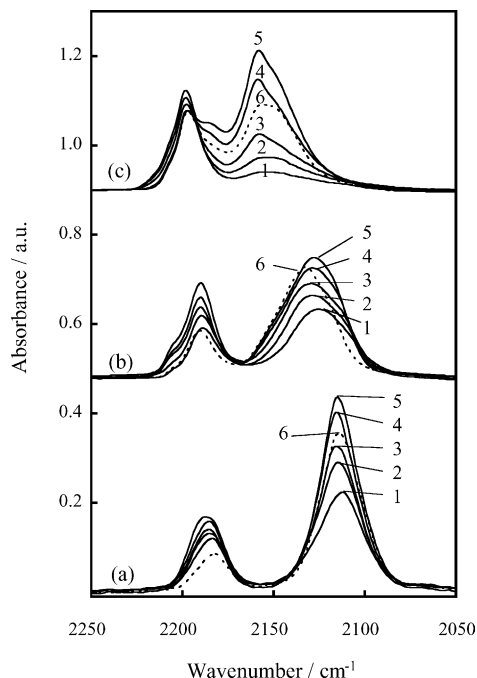


Fig. 4. Reduction of Cu^{II} in samples with the same amount of copper ($0.3 \text{ atoms nm}^{-2}$), and various amounts of sulphates. Copper carbonyls formed upon heating in CO at increasing temperature for 5 min. After the various treatments, all spectra were recorded in the presence of CO at RT. (a) Sample Cu/Z(0.3) exposed to CO at RT (spectrum 1), heated in CO at 393 K (spectrum 2), 423 K (spectrum 3), 453 K (spectrum 4), 503 K (spectrum 5) and 573 K (spectrum 6). (b) Sample Cu/Z(0.3, 1.0) exposed to CO at RT (spectrum 1), heated at 383 K (spectrum 2), 433 K (spectrum 3), 493 K (spectrum 4), 548 K (spectrum 5) and 623 K (spectrum 6). (c) Sample Cu/SZ(0.3, 2.5) exposed to CO at RT (spectrum 1), heated at 413 K (spectrum 2), 493 K (spectrum 3), 573 K (spectrum 4), 623 K (spectrum 5) and 673 K (spectrum 6).

became less intense (Fig. 1b). These results indicate a decreased reducibility of Cu^{II} to Cu^{I} in the presence of sulphates.

In samples with a constant amount of sulphate ($2.5\text{--}2.7 \text{ SO}_4 \text{ nm}^{-2}$), the intensity of the $\text{Cu}^{\text{I}}\text{--CO}$ band was proportional to the copper content from 0.3 to 3.9 Cu nm^{-2} , showing that the fraction of reducible copper did not depend on copper content (Fig. 4 in Ref. [19]), in agreement with previous results on Cu/Z [10,19]. The intensity of the $\text{Cu}^{\text{I}}\text{--CO}$ band was lower on Cu/SZ than on the corresponding Cu/Z, confirming the lower reducibility of Cu^{II} in the presence of sulphates (Fig. 4 in Ref. [19]).

We will examine next the reduction of Cu^{II} upon heating samples in CO at various temperatures. We studied the reduction of Cu^{II} in samples with a constant amount of copper and different amounts of sulphates: Cu/Z(0.3), Cu/Z(0.3, 1.0) and Cu/Z(0.3, 2.5). After the activation procedure, before recording IR spectra in the presence of CO at RT, we heated samples in CO at various temperatures for 5 min. As the temperature of heating in CO increased (i) the band intensity of sulphates remained unchanged (spectra not shown) and (ii) that of $\text{Cu}^{\text{I}}\text{--CO}$ increased, reached a

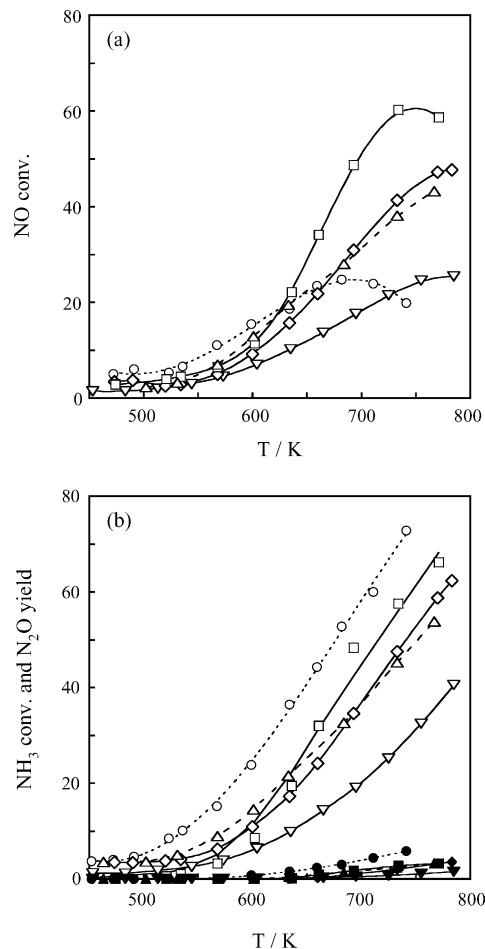


Fig. 5. SCR reaction on samples with the same copper content ($0.3 \text{ Cu atoms nm}^{-2}$), but different sulphate content. Percent NO conversion (a, open symbols), percent NH_3 conversion (b, open symbols) and percent N_2O yield (b, closed symbols) as a function of temperature T (K). Catalysts: Cu/Z(0.3) (\circ , \bullet), Cu/Z(0.3) S_g (0.4) (∇ , \blacktriangledown), Cu/Z(0.3) S_g (0.9) (\diamond , \blacklozenge), Cu/SZ(0.3, 1.0) (\triangle , \blacktriangle) and Cu/Z(0.3) S_g (3.5) (\square , \blacksquare).

maximum intensity and, as the temperature increased further, decreased (Fig. 4). In a previous paper [10], by combining FTIR and volumetric CO adsorption experiments, we demonstrated that the maximum intensity of the $\text{Cu}^{\text{I}}\text{--CO}$ band in Cu/Z(0.3) corresponded to the reduction of all Cu^{II} to Cu^{I} , every Cu^{I} in this sample yielding $\text{Cu}^{\text{I}}\text{--CO}$ (spectrum 5 in Fig. 4a). Because the maximum intensity of the $\text{Cu}^{\text{I}}\text{--CO}$ bands for Cu/Z(0.3, 1.0) and Cu/Z(0.3, 2.5) almost matched that for Cu/Z(0.3), we conclude that also for these two samples all Cu^{II} reduced to Cu^{I} (spectra 5 in Fig. 4). On the sulphated samples, the reduction occurred at higher temperature. As the sulphate content increased, the temperatures at which all Cu^{II} reduced to Cu^{I} were 503 K on Cu/Z(0.3), 548 K on Cu/SZ(0.3, 1.0) and 623 K on Cu/SZ(0.3, 2.5). Sulphates withdraw electrons from O^{\ominus} , thus hampering the reaction $2\text{Cu}^{\text{II}} + 3\text{CO} + \text{O}^{\ominus} \rightarrow 2\text{Cu}^{\text{I}}\text{--CO} + \text{CO}_2$. Namely, the presence of sulphates hinders the reduction of Cu^{II} to Cu^{I} . The presence of sulphates also caused the $\text{Cu}^{\text{I}}\text{--CO}$ band to be larger on the two sulphated

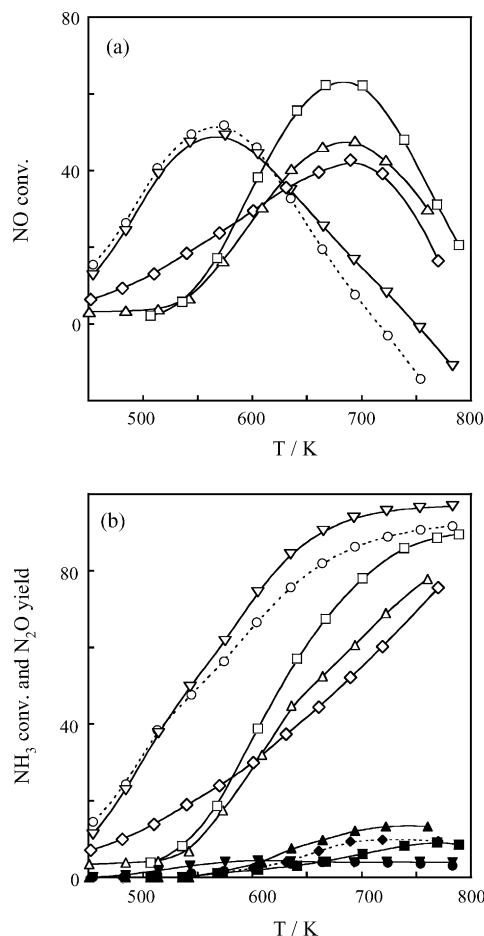


Fig. 6. SCR reaction on samples with the same copper content ($2.5 \text{ Cu atoms nm}^{-2}$), but different sulphate content. Percent NO conversion (a, open symbols), percent NH_3 conversion (b, open symbols) and percent N_2O yield (b, closed symbols) as a function of temperature $T(\text{K})$. Catalysts: $\text{Cu/Z}(2.5)$ (\circ , \bullet), $\text{Cu/Z}(2.5)\text{S}_g(0.3)$ (∇ , \blacktriangledown), $\text{Cu/Z}(2.5)\text{S}_g(1.4)$ (\diamond , \blacklozenge), $\text{Cu/Z}(2.5)\text{S}_g(2.2)$ (\triangle , \blacktriangle) and $\text{Cu/Z}(2.5)\text{S}_g(4.9)$ (\square , \blacksquare).

samples than on $\text{Cu/Z}(0.3)$, owing to the higher heterogeneity of the Cu^{I} species on the sulphated samples. After samples were heated in CO at higher temperature, the decrease of the $\text{Cu}^{\text{I}}\text{--CO}$ band intensity corresponded to the reduction of Cu^{I} to copper metal particles (spectra 6 in Fig. 4).

The results on the Cu^{II} to Cu^{I} reducibility using CO as a reductant agree with those obtained using H_2 by Delahay et al. [25], who showed that the reducibility of Cu^{II} and the oxidability of Cu^{I} both decreased, as the sulphate amount increased [25].

3.3. SCR reaction

3.3.1. Samples with a constant copper amount: the dependence of conversion and selectivity on the sulphate amount

On all catalysts, sulphated or not, increasing the reaction temperature caused NO conversion to reach a maximum and

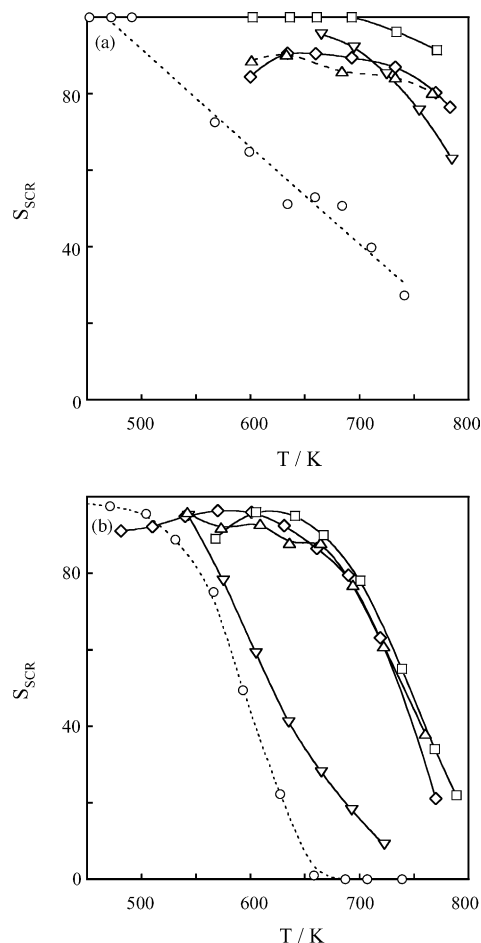


Fig. 7. Percent selectivity S_{SCR} as a function of temperature $T(\text{K})$. Samples with the same copper content (0.3 or $2.5 \text{ atoms nm}^{-2}$), but different sulphate content. (a) $\text{Cu/Z}(0.3)$ (\circ), $\text{Cu/Z}(0.3)\text{S}_g(0.4)$ (∇), $\text{Cu/Z}(0.3)\text{S}_g(0.9)$ (\diamond), $\text{Cu/SZ}(0.3, 1.0)$ (\triangle) and $\text{Cu/Z}(0.3)\text{S}_g(3.5)$ (\square). (b) $\text{Cu/Z}(2.5)$ (\circ), $\text{Cu/Z}(2.5)\text{S}_g(0.3)$ (∇), $\text{Cu/Z}(2.5)\text{S}_g(1.4)$ (\diamond), $\text{Cu/Z}(2.5)\text{S}_g(2.2)$ (\triangle) and $\text{Cu/Z}(2.5)\text{S}_g(4.9)$ (\square).

NH_3 conversion to increase monotonically. The temperature at which NO and NH_3 started to react and the temperature yielding the maximum NO conversion were both higher on the gas-phase sulphated catalysts, $\text{Cu/Z}(0.3)\text{S}_g(b)$ and $\text{Cu/Z}(2.5)\text{S}_g(b)$, than on unsulphated catalysts, $\text{Cu/Z}(0.3)$ and $\text{Cu/Z}(2.5)$ (Figs. 5 and 6). The selectivity S_{SCR} was also higher, remaining higher than 80% up to the temperature yielding the maximum NO conversion (Fig. 7).

Sulphation alone does not determine the catalytic behaviour. At low sulphation extent, (i) $\text{Cu/Z}(2.5)\text{S}_g(0.3)$ and the parent $\text{Cu/Z}(2.5)$ had the same activity and selectivity (Figs. 6 and 7b), whereas (ii) the activity and selectivity of $\text{Cu/Z}(0.3)\text{S}_g(0.4)$ differed markedly from those of the parent $\text{Cu/Z}(0.3)$ (Figs. 5 and 7a). Because the $\text{Cu/Z}(2.5)\text{S}_g(0.3)$ and $\text{Cu/Z}(0.3)\text{S}_g(0.4)$ samples contained similar amounts of sulphate, the two comparisons (i) and (ii) show that another parameter of importance is the sulphate/copper ratio. On $\text{Cu/Z}(0.3)\text{S}_g(b)$ and $\text{Cu/Z}(2.5)\text{S}_g(b)$, as the sulphate content b increased further, the temperature yielding the maximum NO

conversion changed little, NO and NH₃ conversions increased (Figs. 5 and 6), and the S_{SCR} selectivity somewhat increased (Fig. 7). On Cu/Z(0.3)S_g(*b*), as *b* increased from 0.4 to 3.5 SO₄ nm⁻², the apparent activation energy E_a increased from 38 to 62 kJ mol⁻¹. On Cu/Z(2.5)S_g(*b*), as *b* increased from 0.3 to 4.9 SO₄ nm⁻², E_a increased from 39 to 76 kJ mol⁻¹. On Cu/Z(0.3)S_g(*b*) catalysts, the N₂O yield was somewhat lower than on the corresponding Cu/Z(0.3), always remaining lower than 5%. On Cu/Z(2.5)S_g(*b*), the N₂O yield was somewhat higher than on the corresponding Cu/Z(2.5), remaining lower than 15%.

3.3.2. Samples with a constant sulphate amount: the dependence of conversion and selectivity on the copper amount

On Cu/SZ samples, containing the same amount of sulphate (about 2.6 molecules nm⁻²), as the copper amount increased from 0.3 to 3.9 atoms nm⁻², (i) NO and NH₃ conversions increased, (ii) the temperature yielding the maximum NO conversion decreased, (iii) the N₂O yield slightly increased, remaining lower than 10% (Fig. 8) and (iv) the E_a decreased from 79 to 51 kJ mol⁻¹. Up to the temperature yielding the maximum NO conversion, irrespective of the copper content, the selectivity S_{SCR} was higher than 80%. Above this temperature, as the copper content increased, the selectivity S_{SCR} decreased, slightly on Cu/SZ(0.3, 2.5), and markedly on Cu/SZ(1.9, 2.6) and Cu/SZ(3.9, 2.7): at 773 K, S_{SCR} was 75% on Cu/SZ(0.3, 2.5), 55% on Cu/SZ(1.9, 2.6) and 30% on Cu/SZ(3.9, 2.7).

3.4. NH₃ + O₂ reaction

3.4.1. Samples with a constant copper amount: the dependence of activity on the sulphate amount

On all catalysts, sulphated or not, the NH₃ + O₂ reaction yielded NO and a small amount of N₂O, in addition to

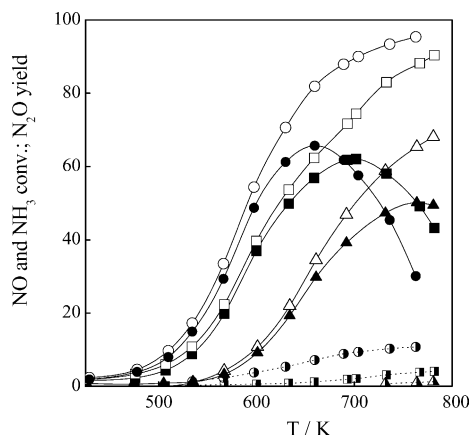


Fig. 8. SCR reaction on samples with the same sulphate content (about 2.6 SO₄ nm⁻²), but different copper content. Percent NO conversion (closed symbols), percent NH₃ conversion (open symbols) and percent N₂O yield (half-closed symbols) as a function of temperature *T*(K). Catalysts: Cu/SZ(0.3, 2.5) (▲, △, ▴), Cu/SZ(1.6, 2.6) (■, □, ▣) and Cu/SZ(3.9, 2.7) (●, ○, ◐).

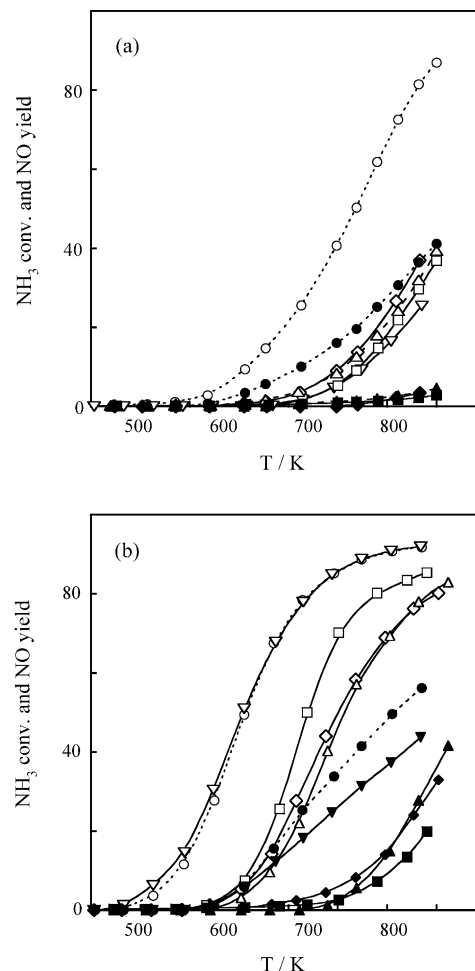


Fig. 9. NH₃ + O₂ reaction on samples with the same copper content (0.3 or 2.5 atoms nm⁻²), but different sulphate content. Percent NH₃ conversion (open symbols) and percent NO yield (closed symbols) as a function of temperature *T*(K). (a) Cu/Z(0.3) (○, ●), Cu/Z(0.3)S_g(0.4) (▽, ▼), Cu/Z(0.3)S_g(0.9) (◇, ◆), Cu/SZ(0.3, 1.0) (△, ▲) and Cu/Z(0.3)S_g(3.5) (□, ■). (b) Cu/Z(2.5) (○, ●), Cu/Z(2.5)S_g(0.3) (▽, ▼), Cu/Z(2.5)S_g(1.4) (◇, ◆), Cu/Z(2.5)S_g(2.2) (△, ▲) and Cu/Z(2.5)S_g(4.9) (□, ■).

N₂. Compared with the unsulphated catalysts, Cu/Z(0.3) and Cu/Z(2.5), on the gas-phase sulphated ones, Cu/Z(0.3)S_g(*b*) and Cu/Z(2.5)S_g(*b*), the light-off of NH₃ shifted to higher temperature and the NO yield was markedly lower (Fig. 9).

As we observed for the SCR reaction, how the catalyst behaves in the NH₃ + O₂ reaction does not depend on sulphation alone. At low sulphation extent, the NH₃ conversion and NO yield (i) were nearly the same on Cu/Z(2.5)S_g(0.3) and on the parent Cu/Z(2.5) (Fig. 9b), whereas (ii) they differed markedly on Cu/Z(0.3)S_g(0.3) and on the parent Cu/Z(0.3) (Fig. 9a). Because Cu/Z(2.5)S_g(0.3) and Cu/Z(0.3)S_g(0.4) had a similar sulphate content, the two comparisons (i) and (ii) show that another influential parameter is the sulphate/copper ratio. On Cu/Z(0.3)S_g(*b*) and Cu/Z(2.5)S_g(*b*), as the sulphate content *b* increased, (i) NH₃ conversions changed little, slightly decreasing on

samples containing 0.3 Cu nm^{-2} and slightly increasing on samples containing 2.5 Cu nm^{-2} , (ii) the NO yield slightly decreased (Fig. 9) and (iii) the N_2O yield slightly increased. On $\text{Cu/Z}(0.3)\text{S}_g(b)$, as b increased from 0.4 to $3.5 \text{ SO}_4 \text{ nm}^{-2}$, E_a increased from 86 to 111 kJ mol^{-1} . On $\text{Cu/Z}(2.5)\text{S}_g(b)$, as b increased from 0.3 to $4.9 \text{ SO}_4 \text{ nm}^{-2}$, E_a increased from 78 to 129 kJ mol^{-1} .

The fact that at any NH_3 conversion, the NO yield in the $\text{NH}_3 + \text{O}_2$ reaction was markedly lower on all Cu/ZS_g than on the relevant Cu/Z accounts for the higher S_{SCR} selectivity observed in the SCR reaction.

3.4.2. Samples with a constant sulphate amount: the dependence of activity on the copper amount

On Cu/SZ samples, containing a constant amount of sulphate (about $2.6 \text{ molecules nm}^{-2}$), as the copper amount increased from 0.3 to $3.9 \text{ atoms nm}^{-2}$ (i) the NH_3 conversions markedly increased, (ii) the NO and N_2O yields increased (Fig. 10) and (iii) the E_a decreased from 118 to 107 kJ mol^{-1} . The increased NO yield in the $\text{NH}_3 + \text{O}_2$ reaction accounts for the S_{SCR} decrease observed in the SCR reaction.

3.5. $\text{NO} + \text{O}_2$ reaction

Cu/Z were active for the $\text{NO} + \text{O}_2$ reaction. The conversion of NO to NO_2 was much higher on $\text{Cu/Z}(2.5)$ than on $\text{Cu/Z}(0.3)$ (Fig. 11). Sulphation via the gas-phase of $\text{Cu/Z}(0.3)$ and $\text{Cu/Z}(2.5)$ caused the NO conversion to decrease markedly in the $\text{NO} + \text{O}_2$ reaction.

At the temperature yielding the maximum NO conversion in the SCR reaction, all catalysts, sulphated or not, were nearly inactive for $\text{NO} + \text{O}_2$, suggesting that the activity for this reaction does not determine the activity in SCR.

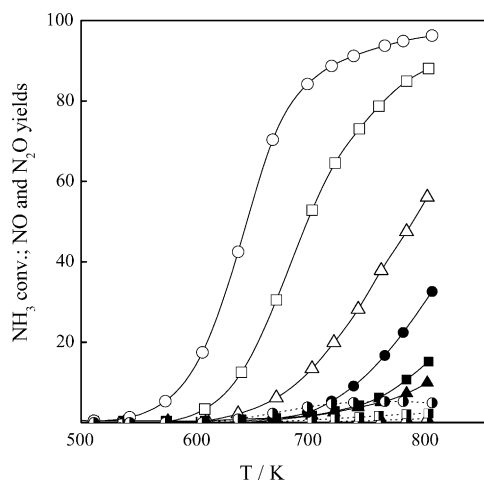


Fig. 10. $\text{NH}_3 + \text{O}_2$ reaction on samples with the same sulphate content (about $2.6 \text{ SO}_4 \text{ nm}^{-2}$), but different copper content. NH_3 conversion (open symbols), NO yield (closed symbols) and N_2O yield (half-closed symbols) as a function of temperature $T(\text{K})$. Catalysts: $\text{Cu/SZ}(0.3, 2.5)$ (Δ , \blacktriangle , \blacktriangle), $\text{Cu/SZ}(1.6, 2.6)$ (\square , \blacksquare , \blacksquare) and $\text{Cu/SZ}(3.9, 2.7)$ (\circ , \bullet , \bullet).

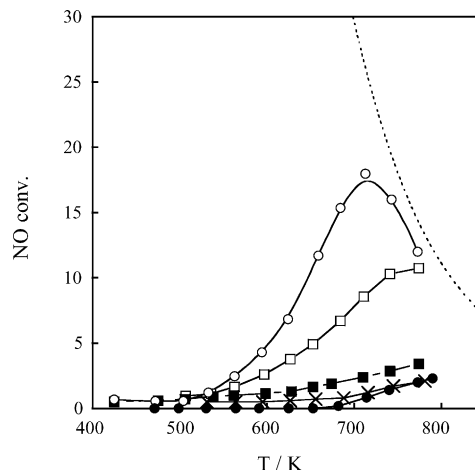


Fig. 11. $\text{NO} + \text{O}_2$ reaction on unsulphated and sulphated $\text{CuO}_x/\text{ZrO}_2$ catalysts. NO conversion as a function of temperature. Catalysts: Z (\times), $\text{Cu/Z}(0.3)$ (\square), $\text{Cu/Z}(0.3)\text{S}_g(0.9)$ (\blacksquare), $\text{Cu/Z}(2.5)$ (\circ) and $\text{Cu/Z}(2.5)\text{S}_g(2.2)$ (\bullet). Dotted line reports the percent NO conversion at equilibrium as a function of temperature.

3.6. The dependence on the preparation method

In the SCR and $\text{NH}_3 + \text{O}_2$ reactions, the catalytic activity of Cu/ZS_g almost equalled that of the corresponding Cu/SZ catalyst, indicating that the two preparation methods were equivalent (compare $\text{Cu/Z}(0.3)\text{S}_g(0.9)$ with $\text{Cu/SZ}(0.3, 1.0)$ in Fig. 5 and in Fig. 9a). We have previously reported that the catalytic activity of the Cu/ZS_g samples almost equalled that of catalysts prepared by impregnation with CuSO_4 [19]. The novel result with Cu/SZ reinforces the point that the three preparation methods (i) sulphation via the gas-phase, (ii) impregnation of SZ with toluene solutions of $\text{Cu}(\text{acetylacetonate})_2$ and (iii) impregnation of Z with aqueous solutions of CuSO_4 led to equivalent catalysts.

4. Conclusions

Neither the activity nor the selectivity of copper containing sulphated- ZrO_2 depends on the sulphation method used in preparing catalysts. How catalysts behave in the SCR and $\text{NH}_3 + \text{O}_2$ reactions does not depend on sulphation alone: another influential parameter is the sulphate/copper ratio.

Our investigation suggests that copper ions and sulphates play distinct roles in determining the activity and selectivity for the SCR reaction. On $\text{CuO}_x/\text{sulphated-ZrO}_2$ with a constant amount of sulphates (about $2.6 \text{ molecules nm}^{-2}$), as the Cu^{II} content increased, the catalytic activity for the SCR reaction and that for the $\text{NH}_3 + \text{O}_2$ reaction increased. Because the activity increase is analogous to that previously observed on $\text{CuO}_x/\text{ZrO}_2$ [11], we conclude that Cu^{II} is the active site for both reactions also when sulphate is present. The presence of sulphates alters the chemical properties of the active Cu^{II} . The presence of covalent sulphates causes

lower reducibility of Cu^{II} , and higher Lewis acid strength of Cu^{I} in $\text{CuO}_x/\text{sulphated-ZrO}_2$ than in $\text{CuO}_x/\text{ZrO}_2$.

Again underlining the distinct role of sulphate, we found that $\text{CuO}_x/\text{sulphated-ZrO}_2$ were less active than the corresponding $\text{CuO}_x/\text{ZrO}_2$ for SCR, $\text{NH}_3 + \text{O}_2$ and $\text{NO} + \text{O}_2$ reactions. In the $\text{NH}_3 + \text{O}_2$ reaction, as the sulphate content increased, the NO yield markedly decreased, thus accounting for the increased S_{SCR} selectivity. In $\text{CuO}_x/\text{sulphated-ZrO}_2$, as the sulphate content increased, copper ions became less prone reversibly to undergo the redox process $\text{Cu}^{\text{II}}/\text{Cu}^{\text{I}}$, thus explaining why catalytic activity and selectivity both depend on the sulphate content.

References

- [1] H. Bosh, F. Janssen, *Catal. Today* 2 (1988) 369.
- [2] G. Busca, L. Lietti, G. Ramis, F. Berti, *Appl. Catal. B: Environ.* 18 (1998) 1.
- [3] J.P. Chen, R.T. Yang, *Appl. Catal.* 80 (1992) 135.
- [4] J.P. Chen, R.T. Yang, *J. Catal.* 139 (1993) 277.
- [5] P. Ciambelli, M.E. Fortuna, D. Sannino, A. Baldacci, *Catal. Today* 29 (1996) 161.
- [6] J. Svachula, N. Ferlazzo, P. Forzatti, E. Tronconi, *Ind. Eng. Chem. Res.* 32 (1993) 1053.
- [7] M.D. Amiridis, I.E. Wachs, G. Deo, J.-M. Jehng, D.S. Kim, *J. Catal.* 161 (1996) 247.
- [8] S.M. Jung, P. Grange, *Catal. Today* 59 (2000) 305.
- [9] S.M. Jung, P. Grange, *Appl. Catal. B: Environ.* 27 (2000) L11.
- [10] V. Indovina, M. Occhiuzzi, D. Pietrogiamomi, S. Tuti, *J. Phys. Chem. B* 103 (1999) 9967.
- [11] D. Pietrogiamomi, D. Sannino, S. Tuti, P. Ciambelli, V. Indovina, M. Occhiuzzi, F. Pepe, *Appl. Catal. B: Environ.* 21 (1999) 141.
- [12] D. Pietrogiamomi, D. Sannino, A. Magliano, P. Ciambelli, S. Tuti, V. Indovina, *Appl. Catal. B: Environ.* 36 (2002) 217.
- [13] G. Xie, Z. Liu, Z. Ahu, Q. Liu, J. Ge, Z. Huang, *J. Catal.* 224 (2004) 36.
- [14] G. Xie, Z. Liu, Z. Ahu, Q. Liu, J. Ge, Z. Huang, *J. Catal.* 224 (2004) 42.
- [15] A. Cimino, D. Cordischi, S. De Rossi, G. Ferraris, D. Gazzoli, V. Indovina, G. Minelli, M. Occhiuzzi, M. Valigi, *J. Catal.* 127 (1991) 744.
- [16] M. Kantcheva, E.Z. Ciftlikli, *J. Phys. Chem. B* 106 (2002) 3941.
- [17] F. Haase, J. Sauer, *J. Am. Chem. Soc.* 120 (51) (1998) 13503.
- [18] C. Morterra, G. Cerrato, V. Bolis, *Catal. Today* 17 (1993) 505.
- [19] V. Indovina, D. Pietrogiamomi, M.C. Campa, *Appl. Catal. B: Environ.* 39 (2002) 115.
- [20] J.R. Ferraro, A. Walker, *J. Chem. Phys.* 42 (1965) 1278.
- [21] M. Waqif, O. Saur, J.C. Lavalley, S. Perathoner, G. Centi, *J. Phys. Chem.* 95 (1991) 4051.
- [22] C. Morterra, L. Orto, C. Emanuel, *J. Chem. Soc. Faraday Trans.* 86 (1990) 3003.
- [23] M. Waqif, M. Lakhdar, O. Saur, J.-C. Lavalley, *J. Chem. Soc. Faraday Trans.* 90 (1994) 2815.
- [24] K. Hadjiivanov, H. Knözinger, *Phys. Chem. Chem. Phys.* 3 (2001) 1132.
- [25] G. Delahay, E. Ensuque, B. Coq, F. Figuéras, *J. Catal.* 175 (1998) 7.